Advances in Synchrotron Radiation

World Scientific
www.worldscientific.com

SYNCHROTRON RADIATION PHOTOELECTRON STUDY OF HEUSLER-TYPE Fe_2VAL-BASED ALLOYS

KAZUO SODA*

Department of Quantum Engineering, Graduate School of Engineering, Nagoya University, Furo-cho, Chikusa-ku, Nagoya 464-8603, Japan

HIDETOSHI MIYAZAKI

Department of Quantum Engineering, Graduate School of Engineering, Nagoya University, Furo-cho, Chikusa-ku, Nagoya 464-8603, Japan

KOJI YAMAMOTO

Department of Quantum Engineering, Graduate School of Engineering, Nagoya University, Furo-cho, Chikusa-ku, Nagoya 464-8603, Japan

TAKAHIRO MOCHIZUKI

Department of Quantum Engineering, Graduate School of Engineering, Nagoya University, Furo-cho, Chikusa-ku, Nagoya 464-8603, Japan

MANABU INUKAI

Department of Quantum Engineering, Graduate School of Engineering, Nagoya University, Furo-cho, Chikusa-ku, Nagoya 464-8603, Japan

MASAHIKO KATO

Department of Quantum Engineering, Graduate School of Engineering, Nagoya University, Furo-cho, Chikusa-ku, Nagoya 464-8603, Japan

SHINYA YAGI

Department of Quantum Engineering, Graduate School of Engineering, Nagoya University, Furo-cho, Chikusa-ku, Nagoya 464-8603, Japan

YOICHI NISHINO

Department of Materials Sciences and Engineering, Nagoya Institute of Technology, Gokiso-cho, Showa-ku, Nagoya 466-8555, Japan

Received (Day Month Year)
Revised (Day Month Year)

The electronic structures of Heusler-type Fe_2VAl-based alloys, *n*-type thermoelectric alloys $Fe_2VAl_{1-z}X_z$ (X = Si, Ge) and *p*-type one $Fe_2(V_{1-y}Ti_y)Al$, have been investigated by photoelectron spectroscopy with use of synchrotron radiation as an excitation photon source. Observed valence-band spectra of Fe_2VAl agree quite well with the predicted density of states with a sharp pseudogap across the Fermi energy E_F. Small substitution in $Fe_2VAl_{1-z}X_z$ and $Fe_2(V_{1-y}Ti_y)Al$

reveals a rigid-band-like energy shift of the valence band, although the observed shift is smaller than expected in the rigid band model. Further substitution causes the modification of the electronic structure near E_F and the appearance of mid-pseudogap states. However, the dependence of the thermoelectric properties of these alloys on substitution can be qualitataively explained by the observed change in the electronic structure near E_F.

Keywords: Fe_2VAl-based alloys; valence-band electronic structure; thermoelectric properties.

1. Introduction

Fe_2VAl-based alloys have received much attention as a potential candidate for new thermoelectric materials.[1] The Heusler($L2_1$)-type ordered alloy Fe_2VAl shows remarkable enhancement of its thermoelectric power by off-stoichiometry or substitution of quaternary elements as well as a semiconductorlike temperature dependence of its electric conductivity over a wide temperature range.[2] For example, the power factor of the substituted alloys $Fe_2VAl_{1-z}Si_z$ exceeds that of typical thermoelectric materials of heavily-doped Bi_2Te_3-based semiconductor.[3] Here, the power factor is one of the thermoelectric figures of merit, defined by

$$P = S^2\sigma\,, \tag{1}$$

where S and σ are the thermoelectric power and electric conductivity of the alloys, respectively. The thermoelectric powers of the substituted alloys fall on a universal curve when they are plotted as a function of an averaged valence electron number per atom, e/a.[1] As for the transport properties, the substitution tends to cause metallic conduction, while Fe_2VAl is in a marginal state between ferromagnetic and nonmagnetic phases and regarded as a candidate of the 3*d* heavy fermion system.[2]

The fascinating thermoelectric properties have been attributed to a sharp pseudogap across the Fermi energy E_F in its electronic structure, which has been theoretically predicted[1,4] and also experimentally confirmed.[5] According to the Boltzmann's transport theory, thermoelectric power $S(T)$ at temperature T may be given by

$$\begin{aligned} S(T) &= \frac{1}{eT}\frac{\int \sigma(E)(E-\mu)\dfrac{\partial f(E)}{\partial E}dE}{\int \sigma(E)\dfrac{\partial f(E)}{\partial E}dE} \\ &\cong \frac{1}{eT}\frac{\int N(E)(E-E_F)\dfrac{\partial f(E)}{\partial E}dE}{\int N(E)\dfrac{\partial f(E)}{\partial E}dE} \\ &\cong -\frac{\pi^2}{3}\frac{{k_B}^2 T}{e}\frac{1}{N(E_F)}\left[\frac{\partial N(E)}{\partial E}\right]_{E=E_F} \end{aligned}\,, \tag{2}$$

where μ, $\sigma(E)$, $f(E)$, and $N(E)$ are the chemical potential ($\mu \cong E_F$ in metals), the electric conductivity at the energy E, the Fermi-Dirac distribution function at T, and the electronic density of states, respectively.[6,7] Thus, we may control the thermoelectric

power through the change in the valence electron concentration induced by the variation in the chemical composition, without the electronic structure of Fe_2VAl altered (the rigid-band behavior). For the Fe_2VAl-based substituted alloys, the dependence of the thermoelectric power on substitution agrees qualitatively well with that estimated by Eq. (2) with the predicted density of states for Fe_2VAl within the rigid-band model, but the maximum or minimum of the thermoelectric power are obtained at smaller substitution than expected, as shown later. Although the enhancement of the thermoelectric power in an off-stoichiometric alloy $(Fe_{2/3}V_{1/3})_{100-y}Al_y$ can be well explained also by the rigid-band model, the shift of the valence band is much smaller than expected in the rigid-band model.[5] Furthermore, an off-stoichiometric alloy $Fe_{2-x}V_{1+x}Al$ shows a large thermoelectric power, whose dependence on the composition x is quite inconsistent with the rigid-band model.[8] These inconsistencies imply the modification of the electronic structure. Not only for the scientific interest but also for the effective development of new thermoelectric materials, it is important to clarify the change in the electronic structure on substitution or off-stoichiometry and its influence on their thermoelectric properties.

In this paper we will report results on the photoelectron spectroscopy of the Heusler-type Fe_2VAl-based alloys, the *n*-type thermoelectric alloys $Fe_2VAl_{1-z}X_z$ (X = Si, Ge) and *p*-type one $Fe_2(V_{1-y}Ti_y)Al$, in order to clarify their electronic structure and its change on substitution. We have found that the dependence of the thermoelectric properties of these alloys on the off-stoichiometry[5] and substitution can be qualitatively explained by the observed change in the electronic structure near E_F. The heavy substitution over about 5 % modifies the electronic structure considerably, while the small substitution shows the rigid-band-like behavior.

2. Experimental

The vacuum ultraviolet photoelectron (UPS) measurement was performed at the beamline BL5U of the 0.75 GeV storage ring, UVSOR-II, at the Institute for Molecular Science by use of linearly polarized vacuum ultraviolet light from an undulator and a spherical grating monochromator and a high-resolution photoelectron energy analyzer (MBS-Toyama A1).[9] The UPS spectra were recorded at 20 K with the total energy resolution of 0.1 eV at the excitation photon energy $h\nu$ of 90 eV. The angle acceptance of the analyzers is about ±8°.

The X-ray photoelectron (XPS) measurement was carried out at the high-resolution photoelectron spectroscopy station of the BL25SU beamline of the 8 GeV electron storage ring, SPring-8, at the Japan Synchrotron Radiation Research Institute using highly monochromatic circularly polarized soft x-ray photons from a twin helical undulator and a spherical grating monochromator as an excitation source.[10] The XPS spectra were recorded at 20 K with a total energy resolution of 0.13 eV at $h\nu$ = 900 eV by use of a hemispherical analyzer (SCIENTA SES200) in the angle integration mode.

Polycrystalline specimens of the Heusler-type Fe_2VAl alloys, $Fe_2VAl_{1-z}X_z$ (X = Si, Ge) and $Fe_2(V_{1-y}Ti_y)Al$, were prepared by repeated arc-melting of appropriate mixtures in an argon atmosphere and subsequent homogenization at 1273 K for more than 48 hours

in a vacuum. After shaping the specimens typically into a size of 1 x 1 x 5 mm^3, they were annealed at 1273 K for an hour and at 673 K for four hours for the $L2_1$ ordering followed by furnace cooling. Chemical composition was determined within an accuracy of ±0.2 atomic % by inductively coupled argon plasma atomic emission spectroscopy. The single phase of the $L2_1$ structure was confirmed by means of x-ray diffraction analysis and transmission electron microscopy.

Clean surfaces for photoelectron measurement were obtained by *in situ* fracturing the specimens with a sharp blade at 20 K under a pressure lower than 1 x 10^{-8} Pa, and were confirmed by measuring the photoelectron spectra in a wide energy range, particularly in a range of the O 1*s* and V 2*p* lines for the XPS measurement. These spectra indicate no carbon and oxygen contamination just after the surface preparation and a very small evolution of the O 1*s* line in 4 hours. No O 2*p*-derived band was observed for the UPS measurement. The spectral shape of the valence band was recognized to be unchanged during the UPS and XPS measurement presented in this article.

The origin of the binding energy E_B, i.e., the Fermi energy E_F, was determined by measuring the Fermi edge of a Au film evaporated onto a sample holding plate. The Au 4*f* core level spectra were also frequently measured for checking and correcting a possible drift of the excitation photon energy in the XPS measurement.

3. Results and Discussion

Typical valence-band spectra of Fe_2VAl are shown in Fig. 1, where excitation photon energies $h\nu$ are indicated and the spectral intensities are normalized with their integrated intensity up to E_B = 10 eV. They are compared with the partial densities of Fe and V 3*d* states calculated by an all-electron full-potential linearlized augumented plane wave (FLAPW) method with the WIEN2k code[12] using the experimental lattice constatnt a = 0.5761 nm.[2] In Fig. 2, we also show the calculated total density of states (DOS), element-decomposed DOS (DOS in the muffin-tin sphere of each element) and simulated photoelectron spectra for comparison. The calculated electronic structure is consistent with results so far reported.[4] The simulated spectra were obtained by multipying the element-and-orbital-angular-momentum-decomposed DOS by the corresponding atomic subshell ionization cross section.[13]

As already reported,[5,11] observed valence-band spectra, in particular XPS spectrum, of Fe_2VAl agree quite well with the predicted density of states, although the UPS spectra near E_F contain fairly large contirbution of the surface layer.[11] Besides the surface effects, the simulated spectra in Fig. 2 clearly indicate the dominance of the transition-metal 3*d* states in the UPS spectra. Thus, the UPS spectra recorded at $h\nu$ = 39 and 52 eV are regarded as representative of the Fe and V 3*d* partial DOS's because of the so-called anti-resonance on the V and Fe 3*p*-3*d* transition, respectively.[15] Observed large intensity near E_F in these anti-resonance spectra is attriburted to the surface effect.[11] The narrowing of the Fe 3*d* bands and the shift of the V 3*d* bands towards the low binding energy side, compared with the calculated DOS or XPS spectrum, may be also ascribed to the surface-layer contribution.[11,14] On the other hand, the XPS spectrum shows remarkable overall

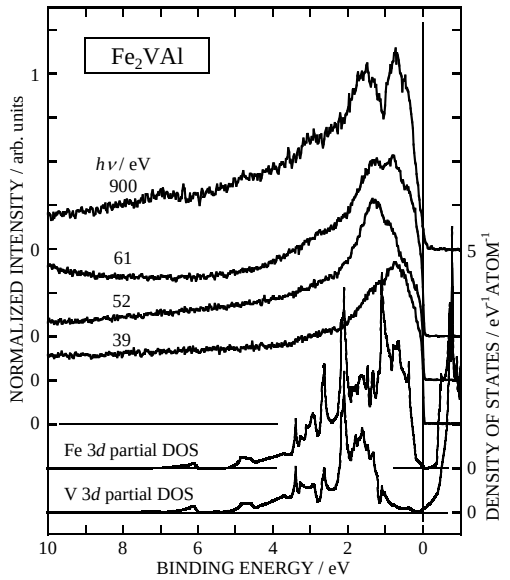

Fig. 1. Typical valence-band photoelectron spectra of Fe_2VAl. Excitation photon energies $h\nu$ are indicated in the figure. Calculated partial densities of Fe and V 3*d* states are also shown for comparison.

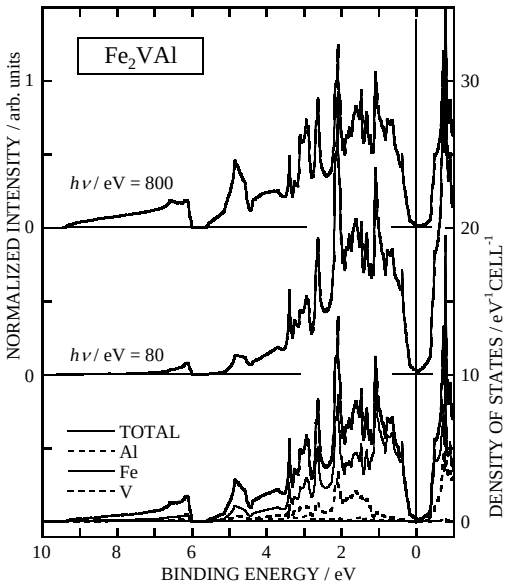

Fig. 2. Calculated density of states and photoelectron spectra of Fe_2VAl.

agreement with the predicted DOS toghether with the steep intensity decrease towards E_F indicating the pseudogap and the appearance of the *sp*-derived bands around E_B = 5 and 7 eV, because of the large bulk-sensitivity of the XPS and the photon energy-dependence

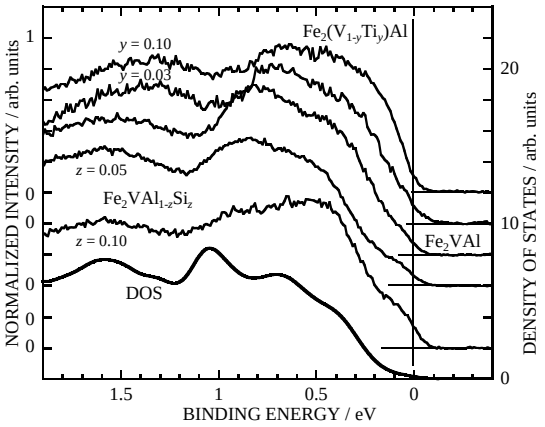

Fig. 3. Typical valence-band XPS spectra of Fe_2VAl-type substituted alloys, $Fe_2(V_{1-y}Ti_y)Al$ and $Fe_2VAl_{1-z}Si_z$. Theoretical density of states is also shown by a thick curve (DOS) after the convolution of a Gaussian function representing experimental energy broadening of 0.13 eV and the Fermi-Dirac distribution function at 20 K.

of the ionization cross section.

Typical XPS spectra near E_F of the *n*-type thermoelectric alloy $Fe_2VAl_{1-z}Si_z$ and *p*-type one $Fe_2(V_{1-y}Ti_y)Al$ are shown in Fig. 3 in comparison with the calculated density of states, which is convoluted with a Fermi-Dirac distribution function and Gaussian function representing the thermal and experimental broadenings, respectively. In Fe_2VAl, there is a shoulder structure near E_F, indicative of the pseudogap, and three Fe and V 3*d*-derived bands at E_B = 0.45, 0.8, and 1.55 eV. The overall features agree well with those in the theoretically calculated DOS, although the experimental spectrum shifts towards the low binding energy side, compared to the theoretical DOS.

On the small substitution of Ti or Si (up to about 5 %), the *d* bands seem shifted as a whole qualitatively along the rigid band model; they are shifted towards the low and high binding energy sides for the *p*-type $Fe_2(V_{1-y}Ti_y)Al$ and *n*-type $Fe_2VAl_{1-z}Si_z$, respectively. The shoulder structure near E_F also becomes prominent on the Si substitution, while it does indistinct on the Ti substitution, as expected in the rigid band model. This rigid-band-like shift results in the enhancement of their thermoelectric power. However, the shift is much smaller than that expected in the rigid band model with the calculated DOS, which may indicate the modification of their electronic structure on substitution or the narrower pseudogap opening than predicted in the band structure calculation. Similar results has been obtained for $Fe_2VAl_{1-z}Ge_z$.[14]

On the large substitution, y = 0.10 and z = 0.10, a shoulder around E_B = 0.25 eV increases its intensity for $Fe_2(V_{1-y}Ti_y)Al$ and a clear new band emerges at about E_B = 0.5 eV for $Fe_2VAl_{1-z}Si_z$. New components are also observed in the constituent core-level spectra for these specimens. These findings suggest a crossover from the rigid-band-like behavior, induced by the substituted element acting as an impurity of the electron or hole donor, to the rearrangement of the electronic structure with new electronic states derived from the substituted element incorporated into the crystal structure.[14]

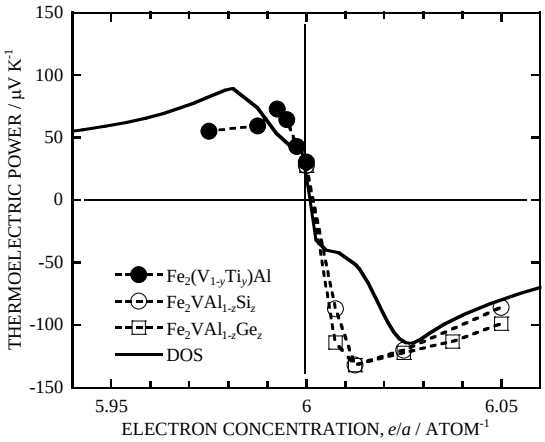

Fig. 4. Thermoelectric power at 300 K of Heusler-type Fe_2VAl-based substituted alloys. Thermoelectric power at 300 K estimated from a theoretical density of states is also shown by a curve (DOS) for comparison.

In Fig. 4, experimental thermoelectric powers at T = 300 K of the investigated alloys[16-18] are compared with those estimated by applying Eq. (2) to the calculated DOS in Fig. 2. For the substituted alloys, the dependence of the thermoelectric power on substitution agrees qualitatively well with the estimated one. However, it is still quantitatively inconsistent with the rigid band model; the thermoelectric power peaks at about a half of the predicted concentration, which corresponds to about 5 % substitution, for both the *n*- and *p*-type alloys. According to the present study, this may be ascribed to the crossover of the electronic structure on substitution; on small substitution up to about 5 % a rigid-band-like energy shift of the valence band enhances thermoelectric power by increasing the energy derivative of $N(E)$ in Eq. (2) because of the sharp pseudogap, while on further substitution the electronic structure near E_F is modified and the pseudogap is destroyed by the appearance of mid-pseudogap states, which may decrease the thermoelectric power. Thus, the dependence of the thermoelectric properties of these alloys on substitution can be qualitataively explained by the observed change in the electronic structure near E_F. Although the X-ray diffraction measurement showed no other phase, the large reduction in the thermoelectric power and large modification of the electronic structure near E_F for $Fe_2(V_{1-y}Ti_y)Al$ on large substitution might arise from an inhomogeneity of the prepared specimens. As for this point, more careful preparation and characterization are necessary for the specimens of the heavily substituted alloys.

4. Summary

We have investigated the electronic structure of the Fe_2VAl-based *p*-type thermoelectric alloy $Fe_2(V_{1-y}Ti_y)Al$ and *n*-type ones $Fe_2VAl_{1-z}X_z$ (X = Si, Ge) in order to clarify the change in their electronic structures on substitution and the correlation between the electronic structure and thermoelectric properties. It is found that the dependence of the thermoelectric properties of these alloys on substitution can be qualitataively explained

by the observed change in the electronic structure near E_F, although the heavy substitution over about 5 % modifies the electronic structure near E_F considerably. The results on photoelectron spectroscopy of the off-stoichiometric alloy $Fe_{2-x}V_{1+x}Al$ will be reported elsewhere in the near future.

Acknowledgments

The XPS measurement was performed at SPring-8 with approval of the Japan Synchrotron Radiation Research Institute (Proposal Nos. 2002A0223-NS-np and 2007A1142). The UPS measurement was supported by the Joint Studies Program of the Institute for Molecular Science (Proposal No. 17-527). This work was partly supported by the Grant-in-Aid for Scientific Research (B) Nos. 13450258 and 17360311 from the Japan Society for the Promotion of Science (JSPS) and also by the Bilateral Joint Research Program between the JSPS and National University of Singapore.

References

1. Y. Nishino, *The Science of Complex Alloy Phases*, ed. T.B. Massalski and P.E. Turchi (TMS, Warrendale, 2005) p. 325.
2. Y. Nishino, M. Kato, S. Asano, K. Soda, M. Hayasaki and U. Mizutani, *Phys. Rev. Lett.* **79**, 1909 (1997).
3. Y. Nishino, *Mater. Sci. Forum* **449-452**, 909 (2004).
4. G. Y. Guo, G. A. Botton and Y. Nishino, *J. Phys. Condens. Matter* **10**, L119 (1998).
5. K. Soda, H. Murayama, K. Shimba, S. Yagi, J. Yuhara, T. Takeuchi, U. Mizutani, H. Sumi, M. Kato, H. Kato, Y. Nishino, A. Sekiyama, S. Suga, T. Matsushita and Y. Saitoh, *Phys. Rev B* **71**, 245112 (2005).
6. T. Takeuchi, T. Kondo, T. Takami, H. Takahashi, H. Ikuta, U. Mizutani, K. Soda, R. Funahashi, M. Shikano, M. Mikami, S. Tsuda, T. Yokoya, S. Shin, *Phys. Rev. B* **69**, 125410 (2004).
7. G. C. McIntosh and A. B. Kaiser, *Phys. Rev. B* **54**, 12569 (1996).
8. T. Nakama, Y. Takaesu, K. Yagasaki, T. Naka, A. Matsushita, K. Fukuda and Y. Yamada, *J. Phys. Soc. Jpn.* **74**, 1378 (2005).
9. *UVSOR Acitvity Report 2004* (Institute for Molecular Science, Okazaki, 2005) p.25.
10. Y. Saitoh, H. Kimura, Y. Suzuki, T. Nakatani, T. Matsushita, T. Muro, T. Miyahara, M. Fujisawa, K. Soda, S. Ueda, A. Sekiyama, S. Imada and S. Suga, *Nucl. Instrum. Methods Phys. Res. A* **467-468**, 553 (2001).
11. H. Miyazaki, K. Soda, S. Yagi, M. Kato, T. Takeuchi, U. Mizutani and Y. Nishino, *J. Vac. Sci. Technol. A* **24**, 1464 (2006).
12. K. Schwarz, P. Blaha, G. K. H. Madsen, *Comp. Phys. Commun.* **147**, 71 (2002).
13. J. J. Yeh and I. Lindau, *Atomic Data Nucl. Data Tables* **32**, 1 (1985).
14. H. Miyazaki, K. Soda, M. Kato, S. Yagi, T. Takeuchi and Y. Nishino, *J. Electron Spectrosc. Relat. Phenom.* **156-158**, 347 (2007).
15. K. Soda, T. Takeuchi, Y. Yanagida, U. Mizutani, M. Kato, Y. Nishino, A. Sekiyama, S. Imada, S. Suga, T. Matsushita and Y. Saitoh, *Jpn. J. Appl. Phys.* **38**, *Suppl.* **38-1**, 496 (1999).
16. H. Kato, M. Kato, Y. Nishino, U. Mizutani and S. Asano, *J. Jpn. Inst. Metals* **65**, 652 (2001).
17. Y. Nishino, S. Deguchi and U. Mizutani, *Phys. Rev. B* **74**, 115115 (2006).
18. H. Matsuura, Y. Nishino, U. Mizutani and S. Asano, *J. Jpn. Inst. Metals* **66**, 767 (2002).